

Supporting Information

Growth of vertically aligned MoS₂ nanosheets on Ti substrate through self-supported bonding interface for high-performance lithium-ion batteries: a general approach

Yu Zhou,^a Yong Liu,^{*a} Wenxia Zhao,^b Fangyan Xie,^b Ruimei Xu,^b Baojun Li,^a Xiang Zhou,^a and Hui Shen^c

^aSchool of Materials Science and Engineering, State Key Laboratory of Optoelectronic Materials and Technologies, Sun Yat-sen University, Guangzhou 510275, China.

*E-mail: liuyong7@mail.sysu.edu.cn.

^bInstrumental Analysis & Research Center, Sun Yat-sen University, Guangzhou 510275, China.

^cInstitute for solar energy system, School of Physics, Sun Yat-sen University, Guangzhou 510275, China.

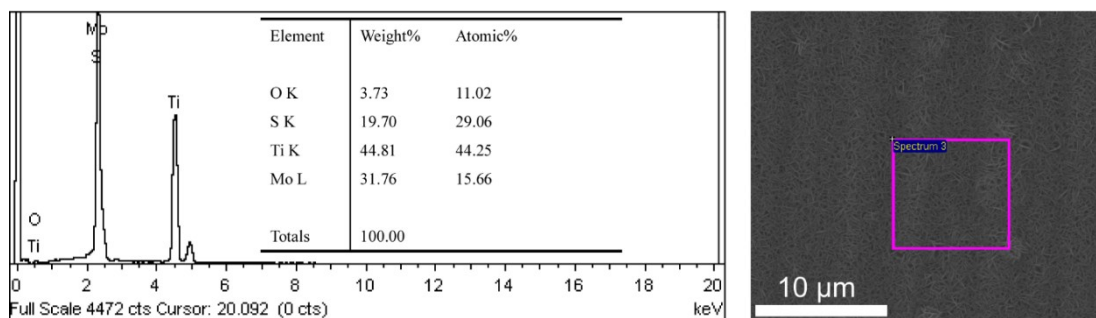


Fig. S1 EDS spectrum of MoS₂ nanosheets grown on the Ti substrate that measured from the pink square circle in right SEM image, inset is a summarized Table of element composition.

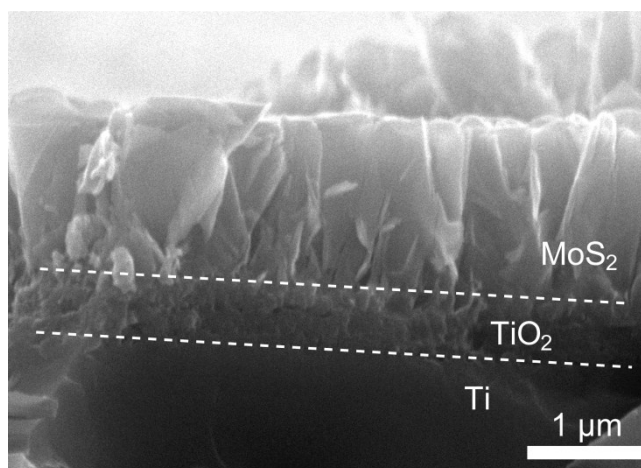


Fig. S2 Cross-sectional SEM images of the fresh MoS₂-230-nanosheet electrode grown on Ti substrate *via* the TiO₂ intermediate layer.

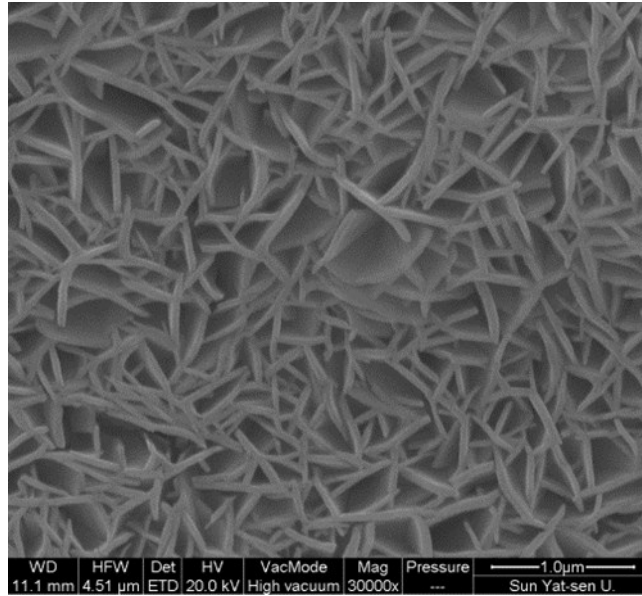


Fig. S3 FESEM image of the MoS₂-230-nanosheet sample after sintering at 800 °C for 2 h.

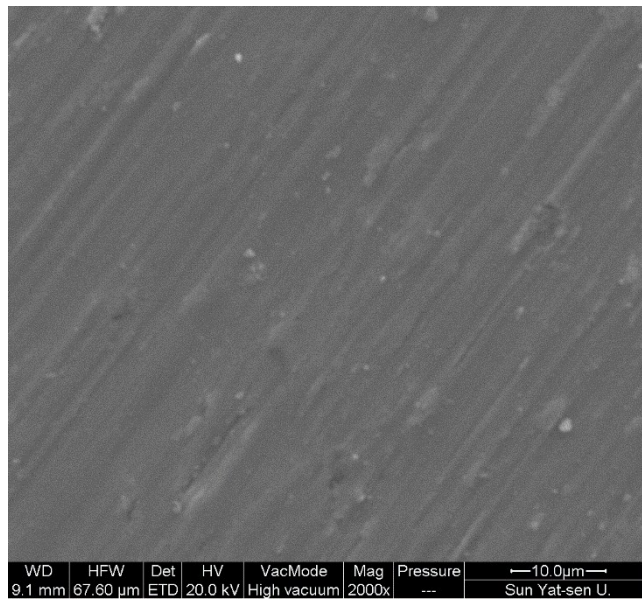


Fig. S4 SEM images of Ti foil with relatively rough surface after being treated with sandpaper dermabrasion.

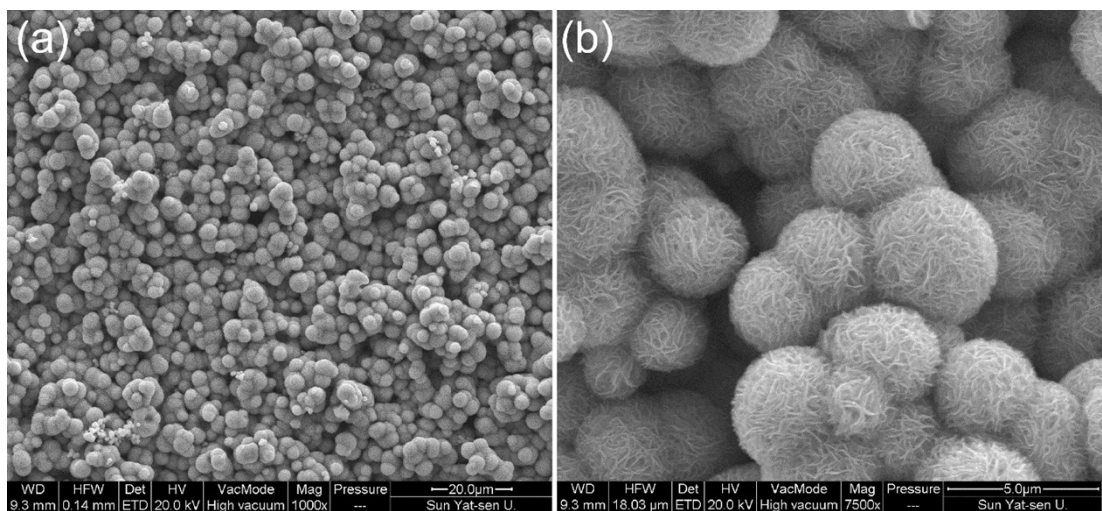


Fig. S5 (a) low magnification and (b) high magnification SEM images of MoS₂ nanosheets assembled hierarchical spheres produced without the addition of ammonia solution, which were collected from the precipitate in the vessel bottom instead of Ti foil.

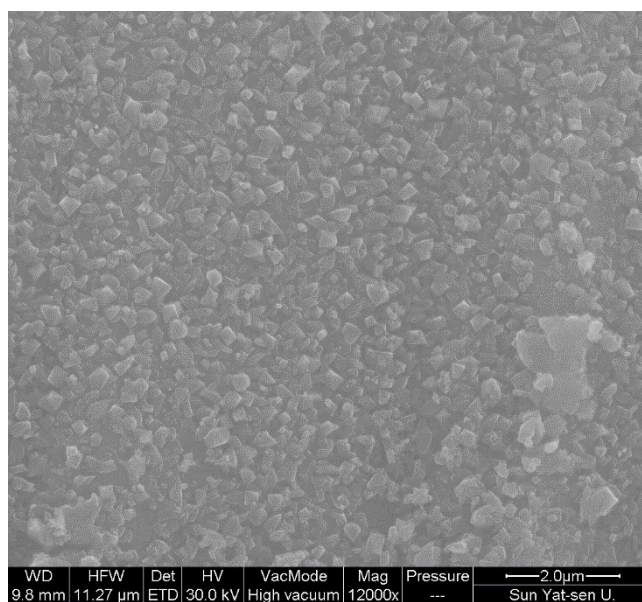


Fig. S6 SEM image of rutile TiO₂ nanocrystals formed on Ti foil, which was obtained in 60 mL ammonia solution at hydrothermal temperature of 230 °C for 24 h without addition of any Mo and S precursors.

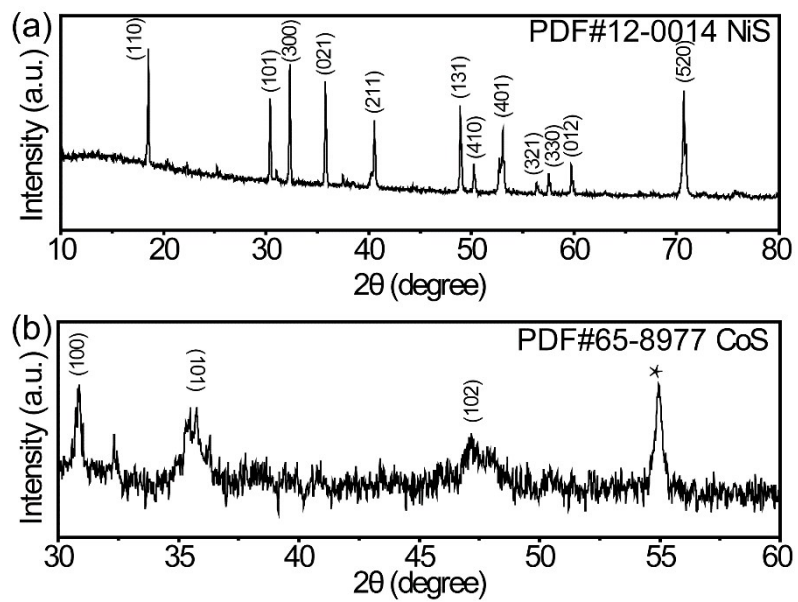


Fig. S7 XRD measurements of other active materials with nanosheet structure grown on Ti substrate. (a) NiS nanosheets, and (b) CoS nanosheets. Some peaks marked with asterisk (*) represent TiO_2 phase.

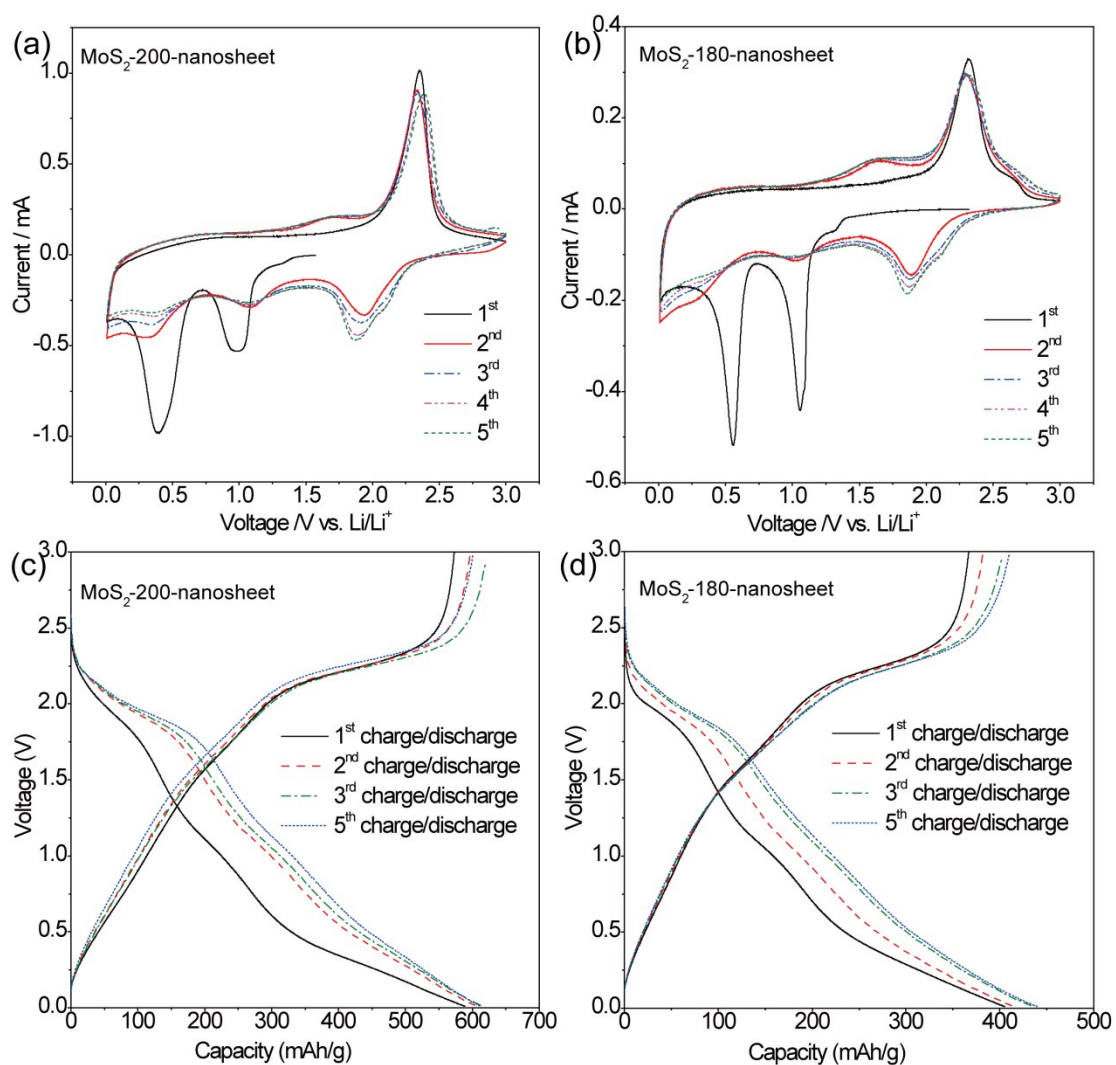


Fig. S8 The represented cyclic voltammetry curves of (a) MoS₂-200-nanosheet electrode and (b) MoS₂-180-nanosheet electrode scanned at 0.5 mV S⁻¹ in a voltage window of 0.01-3.0 V. The charge-discharge voltage profiles of (c) MoS₂-200-nanosheet electrode and (d) MoS₂-180-nanosheet electrode cycled between 0.01 and 3 V (vs Li/Li⁺) at a current density of 100 mA g⁻¹.

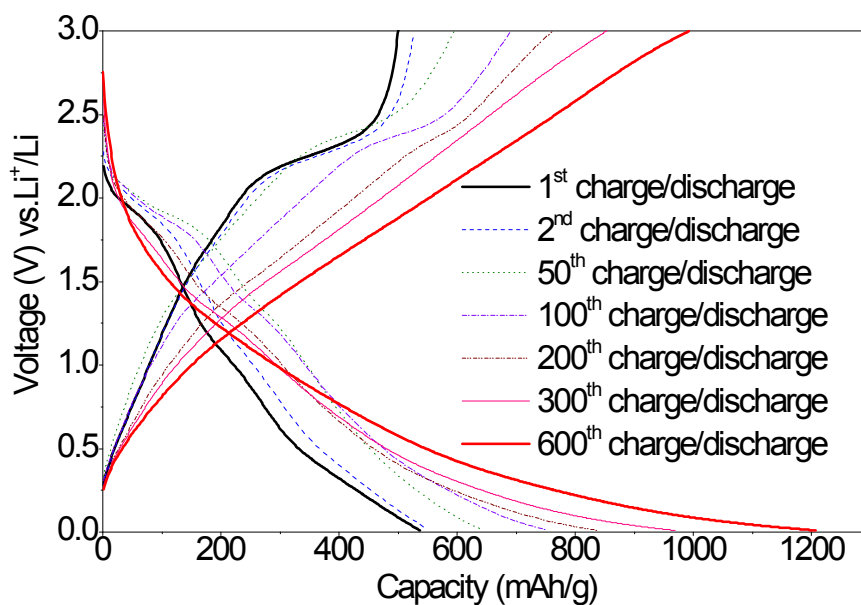


Fig. S9 Voltage profiles of MoS₂-230-nanosheet electrode for the 1st, 2nd, 50th, 100th, 200th, 300th, and 600th cycled between 0.01 and 3 V (vs. Li/Li⁺) at a current density of 1000 mA g⁻¹.

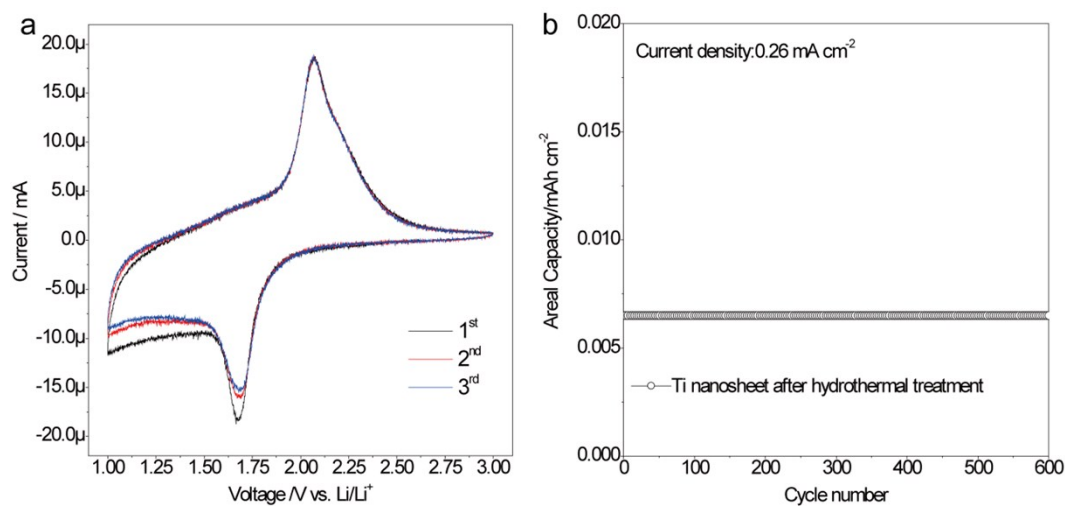


Fig. S10 (a) CV curves and (b) cycling performance of Ti substrate grown with thin TiO₂ layer after hydrothermal treatment without addition of Mo and S sources.

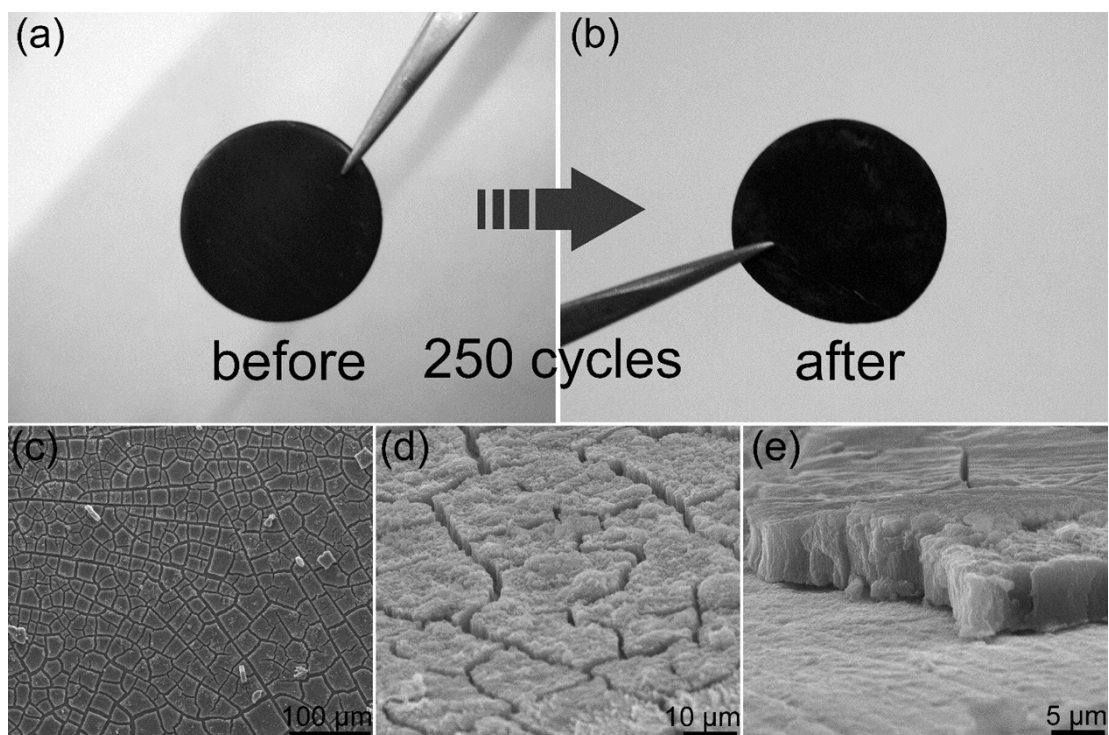


Fig. S11 (a) and (b): Pictures of the MoS₂-230-nanosheet electrode slice before and after 250 discharging/charge process; (c) and (d): Top view and (e) side view SEM images of cycled electrode.

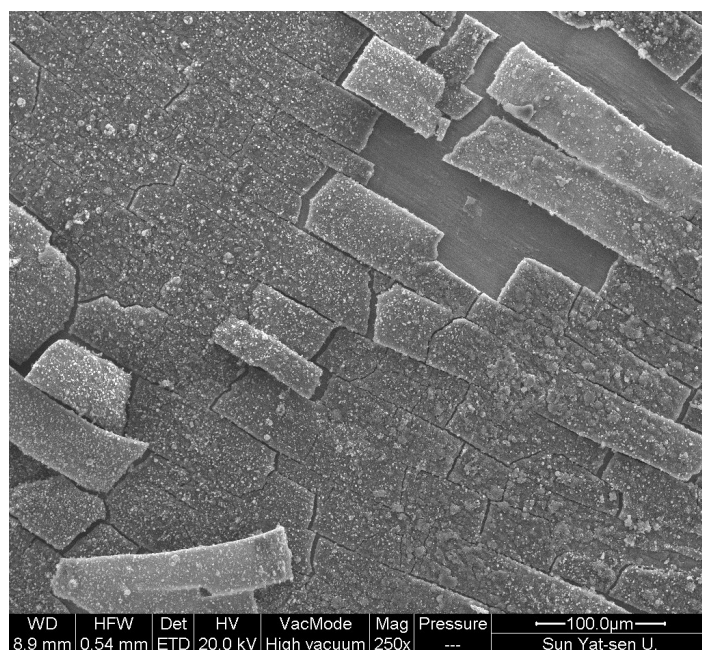


Fig. S12 SEM image of the cycled MoS₂-180-nanosheet electrode after 250 discharging/charge process.

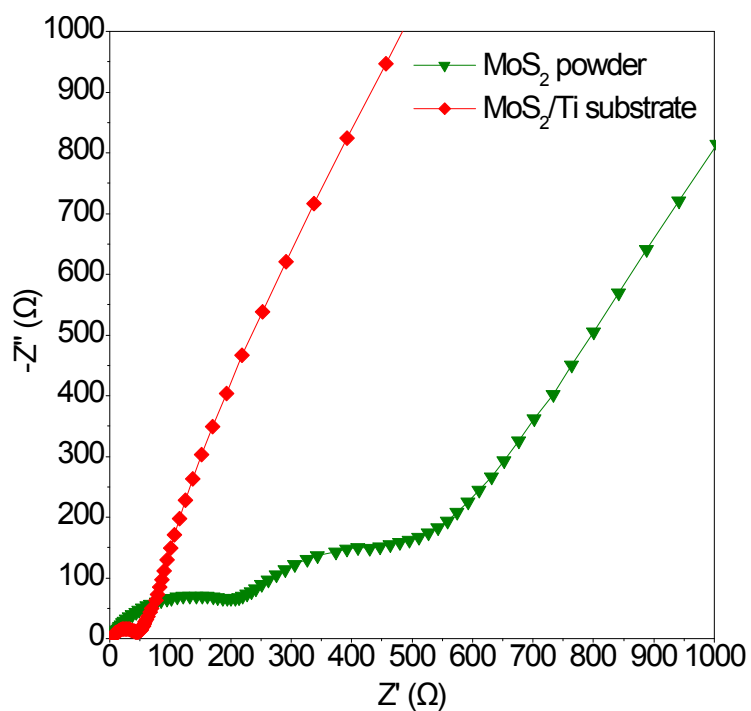


Fig. S13 Nyquist plots of MoS_2 -230-nanosheet electrodes with TiO_2 bonding interface layer and scraped MoS_2 -230-nanosheet electrode without TiO_2 bonding interface layer obtained after 50 discharge/charge cycles at a current rate of 500 mA g^{-1} .

Tab. S1 Kinetic parameters of LIBs constructed by MoS_2 -230-nanosheet, MoS_2 -200-nanosheet, MoS_2 -180-nanosheet and scraped MoS_2 -230-nanosheet electrode after galvanostatic discharging/charging cycles.

Sample	$R_e (\Omega)$	$R_f (\Omega)$	$R_{ct} (\Omega)$
MoS_2 -230-nanosheet	1.5	18.6	37.1
MoS_2 -200-nanosheet	1.8	20.6	44.6
MoS_2 -180-nanosheet	2.0	55.7	77.6
Scraped MoS_2 -230-nanosheet	5.0	204.8	355.3